Chapter 5

Improved Power Angle Control for UPQC-DG in Presence of Unbalanced Load

5.1 Preamble

PAC methods have been effective in optimizing the rating and utilization of UPQC-DG. There have been two types of PAC methods - one based on Instantaneous Reactive Power (IRP or p-q) theory [1, 2] and other based on Synchronous Reference Frame (SRF or d-q) theory [3,4]. Out of the two, SRF based PAC methods have been considered superior due to their robustness against non-ideal grid voltages.

Most of existing PAC methods perform well in presence of balanced loads, but in case of unbalanced loads, they result in circulation of reactive power and thus an improved PAC method has been developed to avoid such situations [5]. In most PAC methods of UPQC-DG it has been proposed that total reactive power demand should be met by series APF (if it is within its capacity) and shunt APF should supply DG power only and shunt APF should supply reactive power only if series APF is not able to supply it fully. This proposition works well in case of balanced loads. However, in case of unbalanced loads, it leads to circulation of reactive power because series APF supplies reactive power equally in all phases. So, applying PAC methods in case of unbalanced loads needs special attention, which has not been given yet in case of UPQC-DG.

Extreme unbalance in loads can cause DC link voltage oscillations of UPQC-DG which deteriorate controller performance. Though good amount of research has been already carried out on control and performance of UPQC in presence of unbalanced loads [6–8], however, little attention is given to DC link voltage oscillations, its effects on performance of UPQC, and solution for it. A sinusoidal integration

block is added to remove DC link voltage oscillations in shunt APF with unbalanced load [9], and a proportional resonant controller is used in place of conventional PI controller [10], but these methods are complex, increase computation burden on controller, and have slow dynamic response.

Therefore, this chapter proposes an improved SRF based PAC method for enhancing performance of UPQC-DG in presence of unbalanced loads to avoid circulation of reactive power and thereby reduce overall kVA loading. Use of a moving average (mean) block at output of PI controller is proposed and analyzed to reduce effect of DC link oscillations. The proposed method has been validated using real time simulation.

The chapter is organized as follows: section 5.2 describes configuration of solar PV based UPQC-DG. Section 5.3 presents analysis of PAC method for UPQC-DG with unbalanced load and section 5.4 covers proposed control method of UPQC-DG using new PAC approach. Section 5.5 presents simulation test case with detailed results and section 5.6 concludes the paper.

5.2 Configuration of UPQC-DG

UPQC-DG configuration, considered in this work, is based on three phase topology of UPQC (Fig. 5.1). Solar PV is selected as DG because of its applicability in India. In UPQC-DG, there are three prominent power converters: series APF, shunt APF and DC-DC converter. Shunt and series APFs are connected through a common DC link. Output of series APF is injected in series with load and source, with help of series injection transformers. Interfacing inductors and RC filters are used at output of both APFs to filter out unwanted switching frequencies. In some cases, DC-DC converter is omitted, but it can lead to sub-optimal PV power generation at low irradiation.

In UPQC-DG configuration, shunt APF injects power available from solar PV into distribution system, eliminating additional solar inverter, which is costly. Filter capacitor, normally used at the output of DC-DC converter, is also not needed.

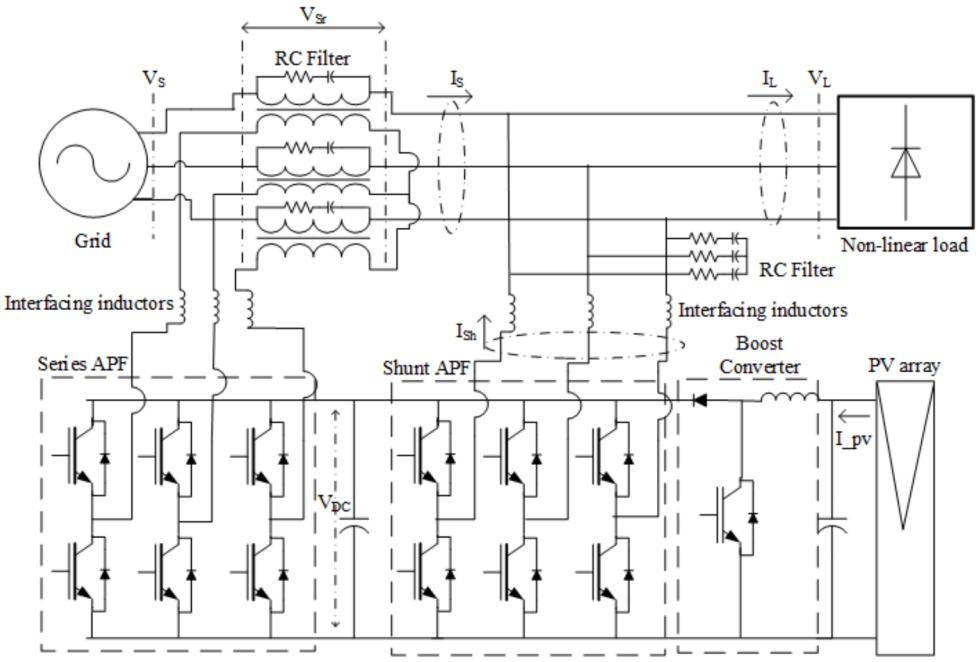

Figure 5.1: UPQC-DG configuration.

5.3 Analysis of PAC Method in case of Unbalanced Load

In this section, an analysis has been presented to show how PAC method can lead to circulation of reactive power and associated increase in VA burden when UPQC-DG compensates for unbalanced load. For simplicity, it is assumed that load reactive power is shared equally between series and shunt APFs ([4]), and DG power injection is zero. Also, it is assumed that series APF supplies a part of unbalanced reactive power (which is more than half of total reactive power of load), which is the condition leading to circulation of reactive power.

Let Q_{La}, Q_{Lb}, Q_{Lc} be three phase reactive power demands of an unbalanced load. Total reactive power of load will be sum of all these (Eq. 5.1). While sharing reactive power equally, series APF will supply half of Q_T (Eq. 6.38). Since series APF can

supply only balanced power, each phase of it will supply $Q_T/6$ (Eq. 5.3).

$$Q_T = Q_{La} + Q_{lb} + Q_{Lc} \tag{5.1}$$

$$Q_{Sr} = Q_T/2 \tag{5.2}$$

$$Q_{Sra} = Q_{Srb} = Q_{Src} = Q_T/6 \tag{5.3}$$

Reactive power supplied by shunt APF in each phase will be difference of load reactive power and series APF power in that phase:

$$Q_{Sha} = Q_{La} - Q_T/6 \tag{5.4}$$

$$Q_{Shb} = Q_{Lb} - Q_T/6 \tag{5.5}$$

$$Q_{Shc} = Q_{Lc} - Q_T/6 \tag{5.6}$$

Let Q_{La} be the least among three phase load reactive powers, then balanced reactive power is given by Eq. 5.7. If load is sufficiently unbalanced then balanced reactive power will be less than half of total reactive power as given by inequality Eq. 5.8, due to which, Q_{Sha} will be negative meaning shunt APF will consume reactive power in phase A, since series APF supplies more reactive power than required. So circulation of reactive power will take place between two APFs.

$$Q_{Bal} = 3Q_{La} \tag{5.7}$$

$$3Q_{La} < Q_T/2 \tag{5.8}$$

When considering total VA power burden on UPQC, magnitude of reactive powers of series and shunt APFs are added. Since Q_{Sha} is negative, its magnitude will be $-Q_{Sha}$. Neglecting active power injections, VA burden of UPQC will be given by Eq. 5.9 and simplified in Eq. 5.10.

$$VA_{UPQC} = (Q_T/6 - Q_{La}) + (Q_{Lb} - Q_T/6) + (Q_{Lc} - Q_T/6) + Q_T/2 \tag{5.9}$$

$$VA_{UPQC} = (Q_T/3 - Q_{La}) + Q_{Lb} + Q_{Lc} \tag{5.10}$$

$$Q_T/3 - Q_{La} > Q_{La} \tag{5.11}$$

$$VA_{UPQC} > Q_{La} + Q_{Lb} + Q_{Lc} \tag{5.12}$$

From inequality Eq. 5.8, inequality Eq. 5.11 can be derived, which proves that VA_{UPQC} is greater than load reactive power (Eq. 5.12). Using above equations it

can be easily seen that if series APF supplies only balanced part of reactive power then there will be no circulation of reactive power and VA_{UPQC} will be equal to load reactive power.

So, During the circulation, one APF supplies reactive power and another APF consumes a part of it, and remaining part goes to load. So total reactive power dealt by of both APFs exceeds load reactive power. This leads to increased VA loading of UPQC-DG. Also, power losses increase due to circulation of currents. So, with unbalanced load, PAC approach of UPQC-DG requires special consideration, which is taken up in this work.

5.4 Proposed Control of UPQC-DG

Control of UPQC-DG is comparatively more complex than control of a conventional UPQC, because of involvement of three converters and DG at DC link. Control of all the three converters of UPQC-DG has been covered in following sub-sections:

5.4.1 Series APF Control

Control of series APF (Fig. 5.3 (a)) using proposed PAC method has been divided in two steps- (1) estimation of power angle (2) generation of switching pulses:

5.4.1.1 Estimation of Power Angle

Phasor diagram for UPQC-DG operating under PAC approach is shown in Fig. 5.2. Quantities with no dash refer to steady state, quantities with single dash refer to sag condition and quantities with double dash refer to swell condition. It can be clearly observed that because of out of phase injection of series voltage, load voltage and source voltage differ by an angle (δ), commonly known in power systems as power angle. Using simple trigonometry, equation for power angle can be obtained:

$$\delta = \cos^{-1}\left[\frac{1+(V_S'/V_S)^2-(V_{Sr}'/V_S)^2}{2V_S'/V_S}\right] \tag{5.13}$$

It can be observed from Fig. 5.2 that power angle increases with increase in series APF voltage. So maximum value of power angle, at a given source voltage (V_S') is achieved when series APF voltage is at its rating:

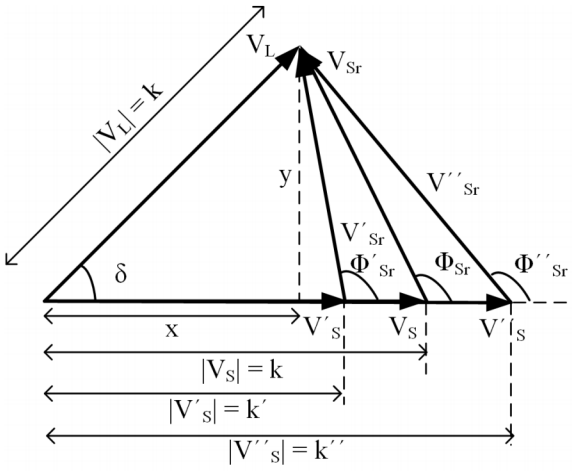

Figure 5.2: Phasor representation of key quantities

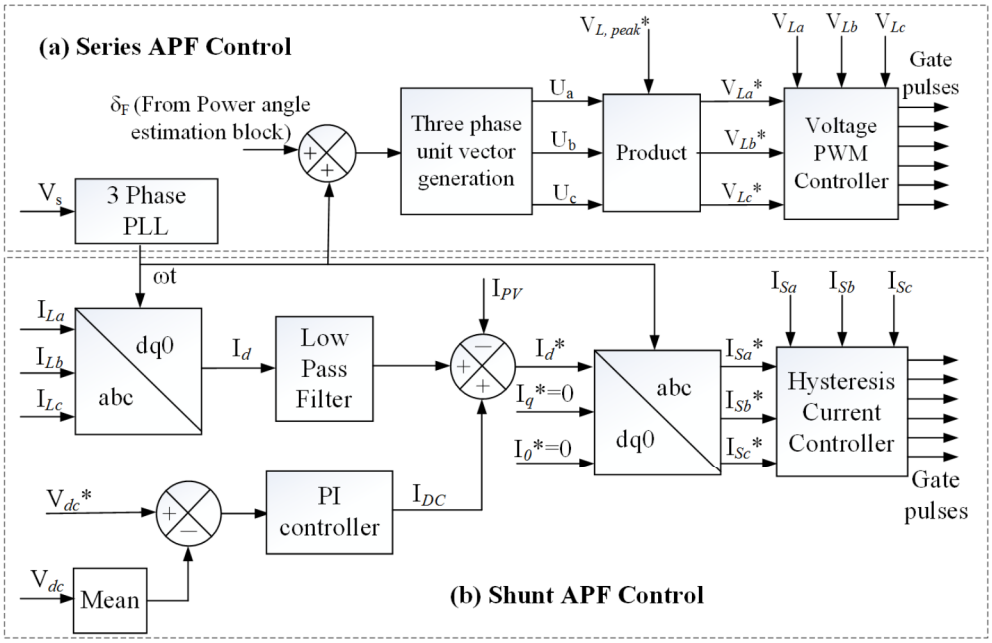

Figure 5.3: PAC based Control of series and shunt APFs of UPQC-DG

$$\delta_{max} = \cos^{-1}\left[\frac{1+(V'_S/V_S)^2-(V'_{Sr,max}/V_S)^2}{2V'_S/V_S}\right] \tag{5.14}$$

Value of maximum power angle for voltage swell condition can be computed in a

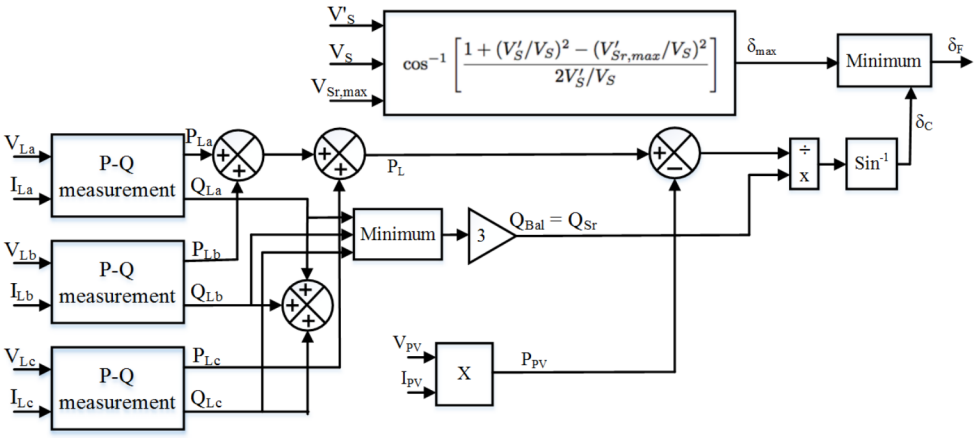

Figure 5.4: Power angle estimation

similar fashion. Instantaneous power angle in case of solar PV based UPQC-DG can be computed from load active and reactive powers , and PV output power (Fig. 5.4):

$$\delta_C = \sin^{-1}\left(\frac{Q_{Sr}}{P_L - P_{PV}}\right) \tag{5.15}$$

As discussed before, series APF should supply only balanced reactive to avoid reactive power circulation and to reduce VA loading of UPQC-DG. Load active and reactive powers are computed for each phase in order to find the balanced part of reactive power. PV output power is estimated using its output voltage and current:

$$P_{PV} = V_{PV} I_{PV} \tag{5.16}$$

In the end, δ_C is compared to δ_{max} and minimum of the two is selected as final power angle (δ_F) for control of series APF.

5.4.1.2 Generation of Switching Pulses

Once power angle has been estimated, next task for series APF is to generate reference load voltages which are leading source voltages by power angle. For this purpose, output of PLL (which is applied on source voltage) is added with power angle and their sum is used to generate three phase unit vectors (Eq. 5.17), which are

in phase with load voltages [11, 12].

$$\begin{bmatrix} U_a \\ U_b \\ U_c \end{bmatrix} = \begin{bmatrix} sin(\omega t + \delta) \\ sin(\omega t + \delta - 2\pi/3) \\ sin(\omega t + \delta + 2\pi/3) \end{bmatrix} \tag{5.17}$$

Reference load voltages are then generated by multiplying the unit vectors with amplitude of reference load voltages. Sensed load voltage signals and reference load voltage signals are then fed to voltage PWM controller of series APF.

5.4.2 Shunt APF Control

Control of shunt APF of UPQC-DG in proposed PAC method is similar to that in conventional PAC method, but compensation of unbalanced loads requires a mean (moving average block) (marked in yellow in Fig. 5.3 (b)) block to be used at output of PI controller. The moving average block removes the undesirable effect of second order ripples of DC link voltage on reference signals generated by the controller. Frequency of the moving average block should be equal to twice the fundamental frequency of grid quantities for improved results [3]. Measured and averaged DC link voltage is compared with constant reference value and error is passed through a PI controller to estimate current (I_{DC}) required for maintaining the DC link voltage.

Effectiveness of the mean block in minimizing second order ripples in I_d^* can be proven mathematically. Let $E_{DC}(t)$ be error input to PI controller. In presence of unbalanced load, $E_{DC}(t)$ will contain second order ripples:

$$E_{DC}(t) = E_0 + E_2 cos(\omega_2 t + \phi_2) \tag{5.18}$$

First term in Eq. 5.18 represents DC component in the error and second term represents ripple component of second order. Current required to maintain DC link voltage ($I_{DC}(t)$) is estimated by PI controller:

$$I_{DC}(t) = K_P E_{DC}(t) + K_I \int_0^t E_{DC}(\tau) d\tau \tag{5.19}$$

From Eq. 5.18 and Eq. 5.19, following equation can be obtained:

$$I_{DC}(t) = K_P E_0 + K_I \int_0^t E_0 d\tau + K_P E_2 cos(\omega_2 t + \phi_2) + K_I \int_0^t E_2 cos(\omega_2 \tau + \phi_2) d\tau \tag{5.20}$$

$$I_{DC}(t) = K_P E_0 + K_I \int_0^t E_0 d\tau + K_P E_2 cos(\omega_2 t + \phi_2) + \frac{K_I E_2 [sin(\omega_2 \tau + \phi_2) - sin\phi_2]}{\omega_2} \quad (5.21)$$

It is clearly seen from Eq. 5.21 that I_{DC} contains second order ripples, which were present in error input of PI controller. If no mean block is used, then these ripples are propagated to I_d^* and deteriorate reference source currents. When mean block (of frequency ω)is used, then mean of DC link current over a running window of $2\pi/\omega$ is given by Eq. 5.22:

$$\bar{I}_{DC}(t) = \frac{1}{2\pi/\omega} \int_t^{t+2\pi/\omega} [K_P E_0 + K_I \int_0^t E_0 d\tau - \frac{K_I E_2 sin\phi_2}{\omega_2}] dt \; + \\ \frac{1}{2\pi/\omega} \int_t^{t+2\pi/\omega} [K_P E_2 cos(\omega_2 t + \phi_2) + \frac{K_I E_2 sin(\omega_2 \tau + \phi_2)}{\omega_2}] dt \quad (5.22)$$

Second term in Eq. 5.22 represents ripples, and it vanishes when $\omega = \omega_2$, since integration of a sinusoidal quantity over its time period is zero. So, A mean block at frequency equal to ripple frequency of DC link, eliminates ripples from I_{DC} and finally, I_d^* also becomes free ripples.

Fundamental and in-phase component of load current is extracted by Park's (d-q) transform (Eq. 5.23) as done in conventional SRF based control of shunt APF. Ramp signal required for d-q transformation is generated by PLL. A low pass filter is used to remove the ripples from generated d-axis current (I_d). Finally reference d-axis current drawn from source is generated by adding I_d & I_{DC} and subtracting I_{PV} (the current generated by solar PV). Reference three-phase source currents are then generated by taking inverse Park's transform.

$$\begin{bmatrix} I_{Ld} \\ I_{Lq} \\ I_{L0} \end{bmatrix} = \frac{2}{3} \begin{bmatrix} sin\omega t & sin(\omega t - \frac{2\pi}{3}) & sin(\omega t + \frac{2\pi}{3}) \\ cos\omega t & cos(\omega t - \frac{2\pi}{3}) & cos(\omega t + \frac{2\pi}{3}) \\ 1/2 & 1/2 & 1/2 \end{bmatrix} \begin{bmatrix} I_{La} \\ I_{Lb} \\ I_{Lc} \end{bmatrix} \quad (5.23)$$

5.4.3 DC-DC Converter Control

Boost converter primarily steps up the output voltage of PV to match with DC link. Secondarily, it ensures extraction of optimum power from PV under varying irradiation and temperature conditions. Out of various existing methods, Incremental Conductance with Integral Regulator (ICIR) MPPT method [13] has been used in this work for control of boost converter. Since it is well known method, its details have been omitted in this chapter.

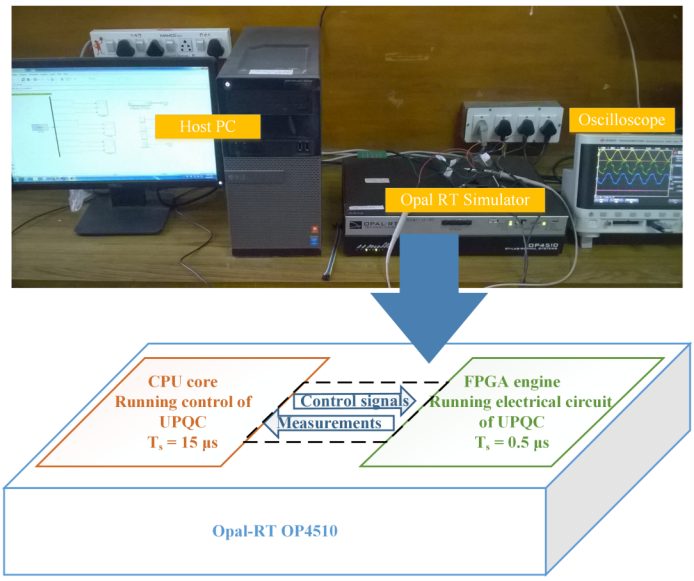

Figure 5.5: Simulation setup

5.5 Real Time Simulation Results

5.5.1 System Data and Simulation Setup

Specifications of UPQC-DG, considered in present work, are given in Table. 5.1. These specifications have been selected based on UPQC-DG design method [14].

Table 5.1: Parameters of UPQC-DG with unbalanced load

3 ϕ supply	415 V, 50 Hz, R_S = .08 Ω, L_S = 0.24 mH
DC link	V_{DC} = 700 V, C_{DC} = 5400 μF
Shunt APF	L_{Sh} = 1.4 mH
Series APF	L_{Sr} = 2.1 mH, n_T = 1, S_T = 2.5 kVA
Boost Converter	545/700 V, L_b = 5 mH
Load-1	diode bridge rectifier (R = 20 Ω, L = 10 mH)
Load-2	R_Y = 9 Ω/phase, L_Y = 6 mH/phase
Load-3	R_{ca} = 10 Ω, L_{ca} = 40 mH
PV array	P_{MPP} = 14.2 KW, V_{MPP} = 550 V

Real time simulation of UPQC-DG system is performed using Opal-RT 4510 simulator in Software in Loop (SIL) configuration (Fig. 5.5). Both plant and controller are simulated in the simulator. Outputs of simulation are obtained on oscilloscope using analog output port of the simulator. In real time simulation, solar PV array has been modeled using equivalent circuit approach [15] and rest of the system has been modeled as shown in Fig. 5.1.

5.5.2 Simulation Results and Discussion

5.5.2.1 Steady State Performance

In steady state, all loads (non-linear, balanced, & unbalanced) are ON. So, load currents are non-linear and unbalanced as shown in Fig. 5.6. The shunt APF compensates these undesired components of load currents and enforces source current to become linear and balanced. THD of source currents is found to be well within 5%, which is acceptable by many power quality standards. Since shunt APF is compensating unbalanced load currents, the currents injected by shunt APF are also unbalanced.

Voltage waveforms in steady state for both proposed PAC and conventional PAC are shown in Fig. 5.7. In proposed PAC, series APF compensates only balanced reactive power (demanded by Load-2), in contrast to conventional PAC, where series APF supplies total reactive power. So, magnitude of series voltage and thus power angle in proposed PAC are less than those in conventional (base case) PAC. Source current is in phase with source voltage in both cases, which shows that net reactive power exchange with grid is zero, however there is circulation of reactive power in base case.

Table 5.2: Comparison of results

Test case	δ (deg)	Shunt APF P_{Sh} (kW)	Q_{Sh} (kVAR)	S_{Sh} (kVA)	Series APF P_{Sr} (kW)	Q_{Sr} (kVAR)	S_{Sr} (kVA)	VA loading of UPQC-DG (KVA)
Base Case	23.1	14.7	6.8	16.2	-1.3	9.1	9.2	25.4
Proposed method	9.4	13.6	9.4	16.5	-0.2	3.5	3.5	20.0

VA loading of both series APF, shunt APF and UPQC-DG (total VA) in both base case and proposed method have been shown in Table. 5.2. Proposed method

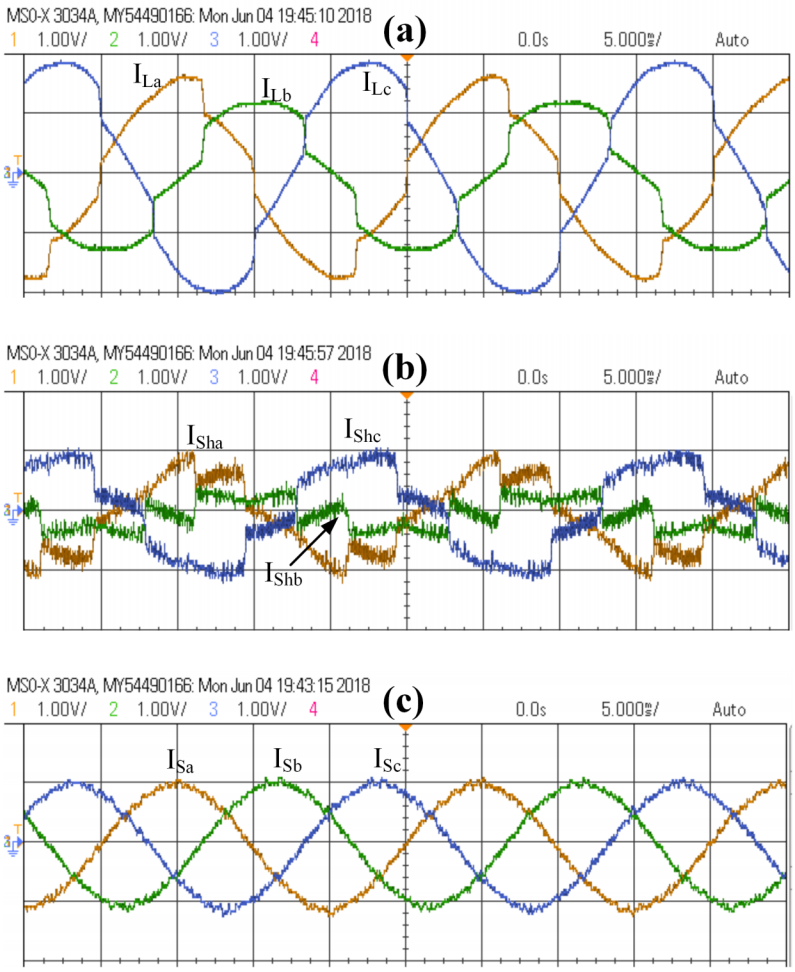

Figure 5.6: Steady state thee-phase currents- (a) three phase unbalanced load currents, (b) three phase compensating currents injected by shunt APF, (c) three phase source currents. Scale- I_L: 50 A/div., I_{Sh}: 50 A/div., I_S: 50 A/div., time: 5 ms/div.

has much less VA loading of series APF in comparison to base case, though VA loading of shunt APF are almost equal. Overall VA loading of UPQC-DG obtained using proposed method is also smaller than that of base case. So, a reduction of 21.1% in VA loading of UPQC-DG is obtained. In proposed method, load reactive power demand equals total reactive power supplied by series and shunt APF together. This indicates that there is no circulation of reactive power in case of proposed PAC method.

Comparison of steady state performance of proposed mean block is done with

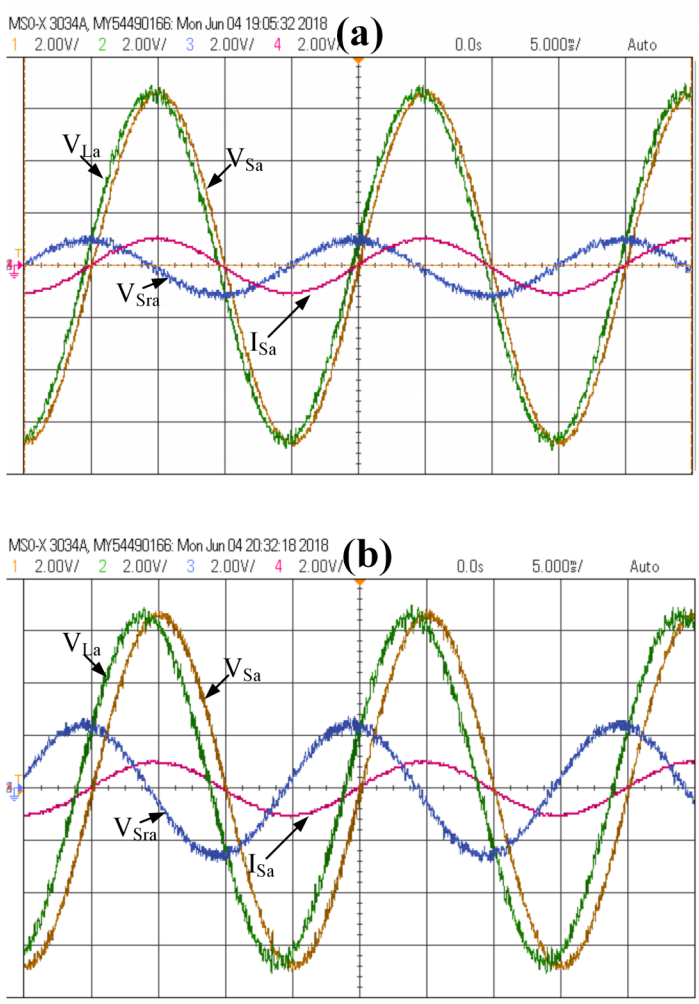

Figure 5.7: Phasor relationships among Steady state waveforms of UPQC-DG (a) in proposed method, (b) in conventional method.
Scale- V_S: 100 V/div., V_L: 100 V/div., V_{Sr}: 100 V/div., I_S: 100 A/div. time: 5 ms/div.

method in which, no mean block is used at the output of PI controller. This comparison is based on two criteria- (1) power quality of source currents and (2) Overall VA burden on UPQC while supplying reactive power of load.

Source current waveforms in base case (without mean block) are shown in Fig. 5.8. It can be observed that in spite of unbalance compensation by shunt APF, certain amount of unbalance remains in source currents. On the contrary, source currents are found to be comparatively much balanced in proposed control (with mean block), as

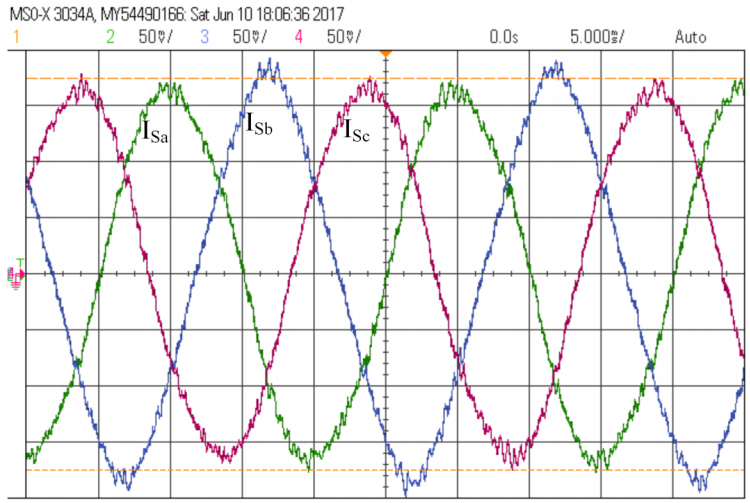

Figure 5.8: Source currents waveforms using method proposed in [4] (Base Case, without mean block)
Scale- I_{Sa}: 50 A/div., I_{Sb}: 50 A/div., I_{Sc}: 50 A/div., time: 5 ms/div.

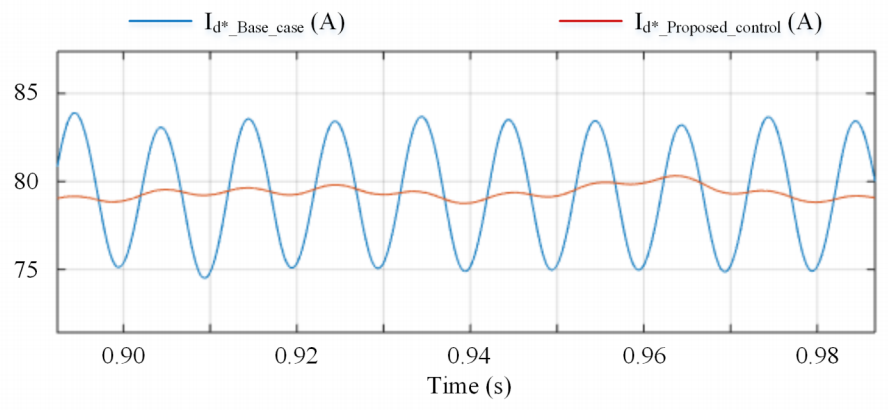

Figure 5.9: Reference d-axis current waveforms in base case (without mean block) and proposed control (with mean block)

already shown in Fig.5.6. To assess power quality of these source currents unbalance and THD are considered for comparison. Source current power quality parameters are presented in Table. 5.3. For comparing unbalance in three phase quantity, percentage unbalance parameter is proposed. Percentage unbalance can be computed using Eq. 5.24.

$$\%Unb = \frac{|I_{a,rms} - I_{b,rms}| + |I_{b,rms} - I_{c,rms}| + |I_{c,rms} - I_{a,rms}|}{I_{a,rms} + I_{b,rms} + I_{c,rms}} \times 100 \qquad (5.24)$$

As evident from Table. 5.3, proposed control performs better in compensating load current unbalance and harmonics. This betterment is due to reduction in ripples in output of PI controller by Mean block and thereby suppression of ripples in reference d-axis source current (Fig. 5.9).

Table 5.3: Comparison of source current power quality using different control methods

S. N.	Method Description	Percentage Unbalance in I_s	THD of I_s
1	No compensation (without UPQC)	27.93%	10.51%
2	Base case (without mean block)	2.66%	4.38%
3	Proposed control (with mean block)	0.11%	3.59%

5.5.2.2 Transient Performance

Transient performance has been tested for following four cases: change in solar irradiation, three phase voltage sag, change in load, and unbalanced voltage sag.

In first case, solar irradiation falling on PV array is reduced from 1000 W/m^2 to 600 W/m^2 (Fig. 5.10(a)). Due to reduction in irradiation, PV current output reduces. So, source current increases. Ideally, shunt APF current should also reduce, but it remains same to compensate for unbalanced load. Load current remains same as if it didn't feel any disturbance due to change in irradiation, which is desired.

In second case of transient study, source voltage is reduced by 25%, a condition typically known as voltage sag (Fig. 5.10(b)). On detection of voltage sag, series APF applies an in-phase voltage to compensate it. Side by side, it keeps supplying reactive power as per its available capacity. So, load voltage remains constant, despite reduction in source voltage. DC link voltage goes through a transient undershoot of 21 V, but settles within 0.14 s. DC link voltage shown in Fig. 5.10 contains ripples, which are due to presence of unbalanced load.

In third case, load change is simulated (Fig. 5.10(c)). Initially load-1 and 2 are ON and load-3 is OFF, and then load-3 is turned ON. As load current increases, source current increases to cater to rise in power demand. Shunt APF current increases to compensate unbalanced currents drawn by load-3.

Performance of proposed UPQC-DG is also validated during an unbalanced source voltage disturbance (Fig. 5.11). A 25% sag is created in phase A of supply voltage,

while voltages of other two phases remain constant. During this disturbance, series APF injects compensating unbalanced voltages, and maintains load voltages constant and balanced. DC link voltage remains constant except for minor undershoot. In comparison to three phase sag, the DC link undershoot is negligible in this case as expected.

5.6 Summary

This chapter proposes a new Power Angle Control (PAC) method for improving performance of UPQC-DG in presence of unbalanced loads. Proposed method avoids circulation of reactive power and reduces overall VA loading of UPQC-DG, while compensating unbalanced loads. Real time simulation in Opal-RT has been performed for validating proposed PAC method. Steady state simulation results show that proposed PAC method reduces VA loading of UPQC-DG by 21.1% in comparison to existing PAC methods. Mean block proposed at output of PI controller is effective in further reducing the unbalance in source currents from 2.66% to 0.11%. Apart from this, proposed method is robust and performs well in dynamic situations such as change in solar irradiation, voltage sag, and change in load.

Bibliography

[1] V. Khadkikar and A. Chandra, "UPQC- S: A novel concept of simultaneous voltage sag/swell and load reactive power compensations utilizing series inverter of UPQC," *IEEE Transactions on Power Electronics*, vol. 26, no. 9, pp. 2414–2425, 2011.

[2] V. Khadkikar, "Fixed and variable power angle control methods for unified power quality conditioner: operation, control and impact assessment on shunt and series inverter kVA loadings," *IET Power Electronics*, vol. 6, no. 7, pp. 1299–1307, 2013.

[3] A. Patel, H. D. Mathur, and S. Bhanot, "A simple approach to improvement in performance of UPQCDG in presence of unbalanced load," in *Proc. 9th IEEE PES Asia-Pacific Power & Energy Engineering Conference*, Oct. 2017, pp. 1–6.

[4] A. K. Panda and N. Patnaik, "Management of reactive power sharing and power quality improvement with SRF-PAC based UPQC under unbalanced source voltage condition," *International Journal of Electrical Power & Energy Systems*, vol. 84, pp. 182–194, 2017.

[5] A. Patel, H. Mathur, and S. Bhanot, "An improved control method for unified power quality conditioner with unbalanced load," *International Journal of Electrical Power & Energy Systems*, vol. 100, pp. 129–138, 2018.

[6] A. J. Viji and T. A. A. Victoire, "Enhanced PLL based SRF control method for UPQC with fault protection under unbalanced load conditions," *International Journal of Electrical Power & Energy Systems*, vol. 58, pp. 319–328, 2014.

[7] I. Axente, J. N. Ganesh, M. Basu, M. F. Conlon, and K. Gaughan, "A 12-kva dsp-controlled laboratory prototype UPQC capable of mitigating unbalance in source voltage and load current," *IEEE Transactions on power Electronics*, vol. 25, no. 6, pp. 1471–1479, 2010.

[8] M. Kesler and E. Ozdemir, "Synchronous-reference-frame-based control method for UPQC under unbalanced and distorted load conditions," *IEEE Transactions on Industrial Electronics*, vol. 58, no. 9, pp. 3967–3975, 2011.

[9] L. Limongi, D. Roiu, R. Bojoi, and A. Tenconi, "Analysis of active power filters operating with unbalanced loads," in *Proc. IEEE Energy Conversion Congress and Exposition*. IEEE, 2009, pp. 584–591.

[10] P. Dang and J. Petzoldt, "A new control method for eliminating the 2nd harmonic at the dc link of a shunt APF under an unbalanced and nonlinear load," in *Power Electronics and Applications (EPE 2011), Proceedings of the 2011-14th European Conference on*. IEEE, 2011, pp. 1–5.

[11] A. Patel, H. D. Mathur, and S. Bhanot, "A new SRF-based power angle control method for UPQC-DG to integrate solar PV into grid," *International Transactions on Electrical Energy Systems*, vol. 29, no. 1, p. e2667, 2019.

[12] V. Khadkikar, P. Agarwal, A. Chandra, A. Barry, and T. Nguyen, "A simple new control technique for unified power quality conditioner (UPQC)," in *Proc. 11th IEEE International Conference on Harmonics and Quality of Power*, 2004, pp. 289–293.

[13] M. Abdulkadir, A. Samosir, and A. Yatim, "Modelling and simulation of maximum power point tracking of photovoltaic system in Simulink model," in *Proc. IEEE International Conference on Power and Energy*, 2012, pp. 325–330.

[14] S. Devassy and B. Singh, "Design and performance analysis of three-phase solar PV integrated UPQC," *IEEE Transactions on Industry Applications*, vol. 54, no. 1, pp. 73–81, 2018.

[15] M. G. Villalva, J. R. Gazoli, and E. Ruppert Filho, "Comprehensive approach to modeling and simulation of photovoltaic arrays," *IEEE Transactions on Power Electronics*, vol. 24, no. 5, pp. 1198–1208, 2009.

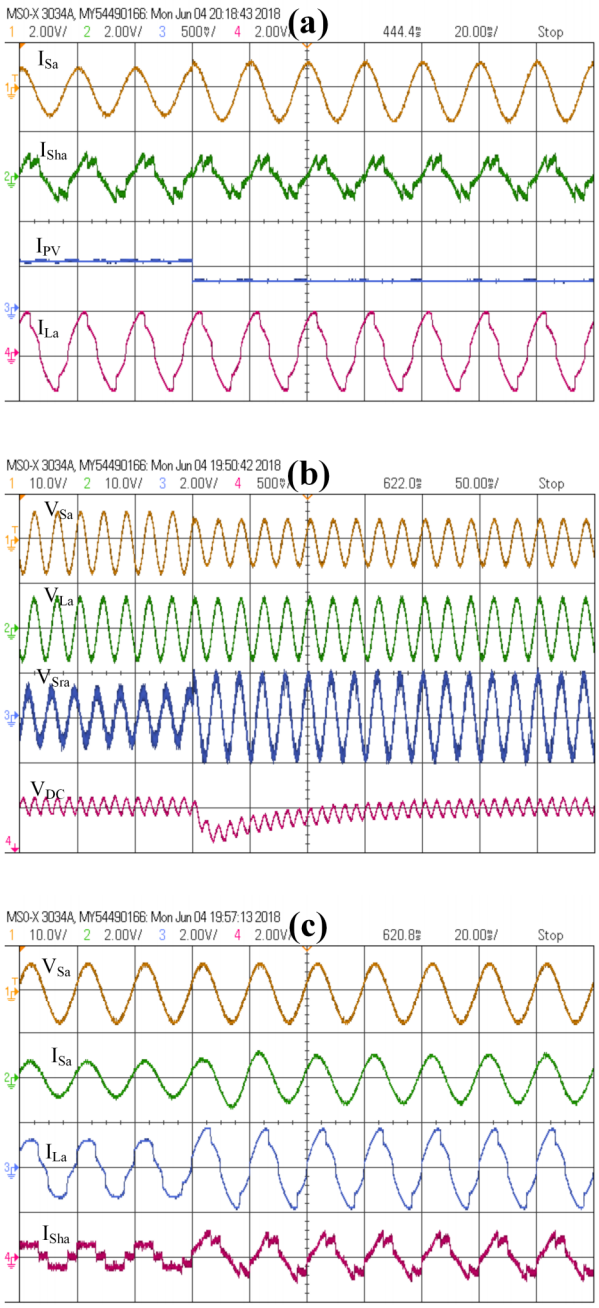

Figure 5.10: Transient waveforms- (a) Waveforms during change in solar irradiation, (b) Waveforms during sag, (c) Waveforms during change in load
Scale- I_S: 100 A/div., I_L: 100 A/div., I_{Sh}: 100 A/div., I_{PV}: 25 A/div., V_S: 500 V/div., V_L: 500 V/div., V_{Sr}: 100 V/div., V_{DC}: 25 V/div., time: 20, 50 ms/div.

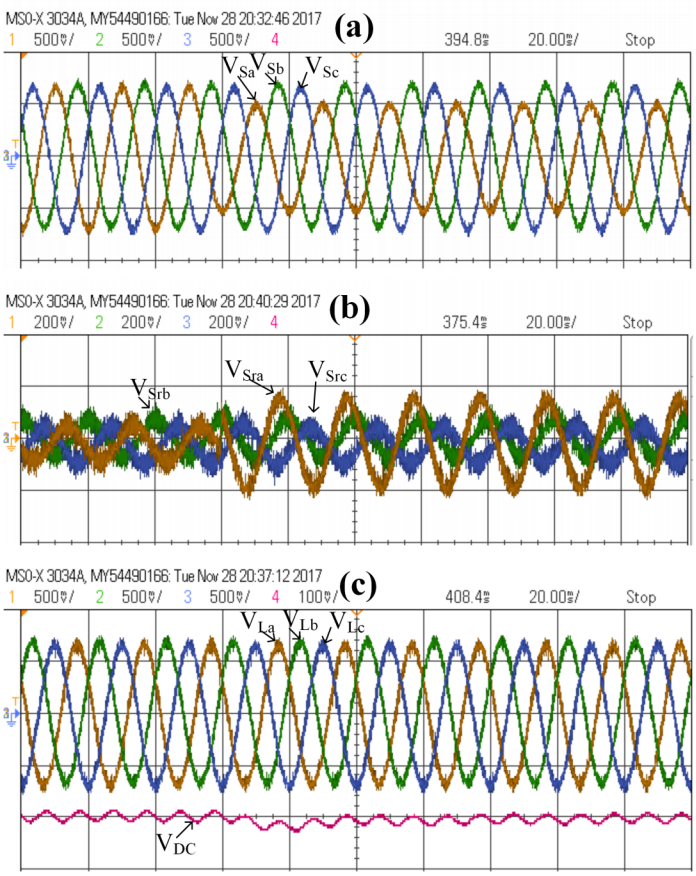

Figure 5.11: Waveforms during unbalanced sag in supply voltage- (a) Three phase source voltages, (b) Three phase voltages injected by series APF, (c) Three phase load voltages and DC link voltage
Scale- V_S: 250 V/div., V_{Sr}: 100 V/div., V_L: 250 V/div., V_{DC}: 50 V/div., time: 20 ms/div.